

# Jamming and percolation properties of random sequential adsorption with relaxation

Sumanta Kundu,<sup>1,\*</sup> Nuno A. M. Araújo,<sup>2,†</sup> and S. S. Manna<sup>1,‡</sup>

<sup>1</sup> *Satyendra Nath Bose National Centre for Basic Sciences, Block-JD, Sector-III, Salt Lake, Kolkata-700106, India*

<sup>2</sup> *Departamento de Física, Faculdade de Ciências, Universidade de Lisboa, 1749-016 Lisboa, Portugal*

The random sequential adsorption (RSA) model is a classical model in Statistical Physics for adsorption on two-dimensional surfaces. Objects are deposited sequentially at random and adsorb irreversibly on the landing site, provided that they do not overlap any previously adsorbed object. The kinetics of adsorption ceases when no more objects can be adsorbed (jamming state). Here, we investigate the role of post-relaxation on the jamming state and percolation properties of RSA of dimers on a two-dimensional lattice. We consider that, if the deposited dimer partially overlaps with a previously adsorbed one, a sequence of dimer displacements may occur to accommodate the new dimer. The introduction of this simple relaxation dynamics leads to a more dense jamming state than the one obtained with RSA without relaxation. We also consider the anisotropic case, where one dimer orientation is favored over the other, finding a non-monotonic dependence of the jamming coverage on the strength of anisotropy. We find that the density of adsorbed dimers at which percolation occurs is reduced with relaxation, but the value depends on the strength of anisotropy.

## I. INTRODUCTION

Adsorption of geometrical objects on a substrate has been a problem of great interest due to its applicability in a variety of fields ranging from photonic crystals to quantum dots including, e.g., surface coating and encapsulation [1–8]. Theoretically, the model of Random Sequential Adsorption (RSA) has been studied intensively over last decades in the context of irreversible processes of adsorption on surfaces [9–11]. P. J. Flory introduced the RSA model in a one-dimensional chain to study the interaction between blocks along a linear polymer chain [12]. This model attracted great attention from the scientific community and was later interpreted as a problem of critical phenomena by Rényi [13] and Feder [14].

In RSA, the objects are adsorbed sequentially and irreversibly at randomly selected vacant positions on a surface. Selection of occupied positions are discarded due to the excluded volume interaction with the previously adsorbed objects. These objects are assumed to be inherently immobile, i.e., they never move out from their positions after adsorption. The interesting feature of this model is the existence of a non-trivial jamming state where no more objects can be adsorbed [5, 15].

Subsequently, a number of variants of the RSA model have been studied to explain the observations of various natural and experimental scenarios [5, 16–21]. For example, the model of accelerated RSA was introduced to describe the mechanism of precursor mediated chemisorption [17]. In this model, if the deposited object lands on top of the already adsorbed objects it starts diffusing till it finds a vacant gap where it is adsorbed irreversibly [18].

The configuration of objects at any arbitrary interme-

diated stage of the RSA process corresponds to a disordered system and the study of their percolation properties [22–29] is of interest. To describe briefly, in percolation the sites (bonds) of a regular lattice are occupied with probability  $p$  or kept vacant with probability  $(1 - p)$ . These occupied sites (bonds) form clusters of different sizes through their neighboring connections. A continuous transition between the ordered and disordered phases is observed at a critical value of  $p = p_c$ . For  $p > p_c$ , there exists global connectivity through macroscopic cluster that scales linearly with the volume of the system. Numerically, this usually the one that spans between two opposite sides of the lattice [23]. Till date, the best value of  $p_c$  for the site percolation on the square lattice is 0.59274605079210(2) [30] and exactly 1/2 for the bond percolation.

In this paper, we introduce a variant of RSA where the objects (dimers) are adsorbed irreversibly onto the lattice sites after going through a well defined relaxation dynamics. We consider a very simple relaxation dynamics where, during the relaxation, a series of dimer displacements may occur to accommodate the new dimer. The effect of such a relaxation dynamics and anisotropy in the orientation of the adsorbed dimers on the jamming state and percolation transition are investigated here using numerical simulations.

## II. MODEL

Dimers are adsorbed sequentially at random positions onto an initially empty square lattice of size  $L \times L$ , with periodic boundary condition. Each dimer occupies two lattice sites. To attempt the adsorption of a dimer, its orientation (either vertical or horizontal) is first selected randomly with equal probability for both orientations. A pair of neighboring sites are then selected accordingly at random and the dimer is deposited on them.

Depending on the occupation state of the pair of sites,

\*sumanta492@gmail.com

†nmaraujo@fc.ul.pt

‡subhrangshu.manna@gmail.com

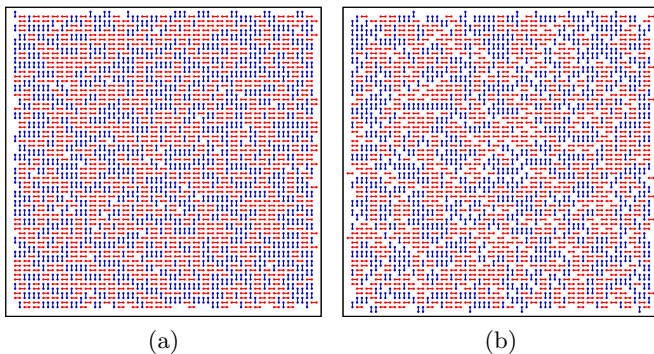


FIG. 1: Typical jamming state configuration of the dimers on a  $64 \times 64$  square lattice for the Random Sequential Adsorption model (a) with and (b) without relaxation. The dimers oriented in the horizontal and vertical directions have been painted in red and blue colors, respectively. The single vacant sites are represented by white color.

there are three possible outputs. First, if the pair of sites are both occupied by previously adsorbed dimers, adsorption fails. Second, if both sites are vacant, the adsorption is successful and the dimer is irreversibly adsorbed on them. Third, if only one of the sites is vacant, a sequence of dimer displacements is triggered, described as follows. When the deposited dimer (A) overlaps with a previously adsorbed dimer (B) at one end, the dimer B is displaced by a unit distance along its other end, keeping A fixed. The displaced dimer may partially overlap with another dimer (C) leading to similar displacement of C. The system of adsorbed dimers thus relaxes and eventually reaches a stable state when no more overlapping of dimers exists. This concerted move completes the “successful” adsorption of dimer A through a relaxation process. Here one assumes the existence of two infinitely separated time scales, as we consider that the relaxation process is always faster than the inter-arrival time of deposited particles. The trail of dimer displacements originated by depositing A constitute a path which is referred as the “relaxation path”. It has been observed that often a relaxation path forms a closed loop. In such a case, the deposition attempt fails and the deposited dimer is discarded. The sequence of dimer adsorption attempts is continued till a jamming state is reached, where no more dimers can adsorb.

The coverage of the surface is defined as  $p = 2n/L^2$ , where  $n$  is the number of adsorbed dimers. An occupied site can never become vacant, since there are no desorption events during the relaxation. When  $p$  is small, adsorption of dimers is mainly uncorrelated and post-relaxation is negligible. For intermediate values of  $p$ , successful adsorptions are often associated with relaxation. In this case, the newly occupied pair of sites are positioned at the two ends of the relaxation path and are separated by a distance larger than unity. Thus, the relaxation process introduces spatial correlations between

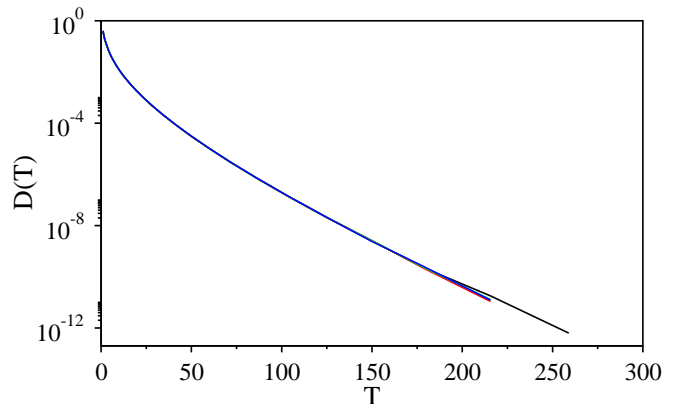


FIG. 2: Plot of the binned data of the relaxation time distribution  $D(T)$  for the entire process of adsorption on a log-linear scale using the lattice sizes  $L = 256$  (black), 512 (red), 1024 (green), and 2048 (blue). The data points are averages over samples ranging from  $2 \times 10^6$  for  $L = 256$  to 12000 for  $L = 2048$ .

occupied sites. Such a source of correlation is absent in the model of RSA without relaxation. By further increasing the value of  $p$ , the clusters of occupied sites start merging leading to a percolation transition. The percolation threshold  $p_c$  is defined as the minimum value of  $p$  for which a giant cluster emerges that spans the entire surface, touching opposite ends of the lattice. This percolation transition is observed before the jamming transition.

### III. RESULTS

#### A. Jamming state and relaxation time

The averaged fraction of the occupied sites at the jamming state defines the jamming coverage  $p_j$ . Figure 1(a) depicts a typical jamming state configuration of RSA model with relaxation and we compare it with one obtained for RSA without relaxation, Fig. 1(b). The relaxation dynamics promotes the reorganization and packing of the dimers more densely so that the jamming state coverage is larger than that of the RSA without relaxation. Numerically, we have estimated the jamming state coverage  $p_j(L)$  and its standard deviation  $\Delta(L) = ((p_j^2) - \langle p_j \rangle^2)^{1/2}$  for different system sizes  $L = 256, 512, 1024, 2048$ , and 4096. We observe no significant finite-size effects for  $p_j(L)$  and that its value is 0.99049(3) compared to 0.90682(3) for RSA without relaxation. The value of  $\Delta(L)$  indeed varies significantly with  $L$ . Fitting to a power-law decay:  $\Delta(L) \sim L^{-1/\nu_j}$  we have estimated  $\nu_j = 1.002(3)$ , consistent with a linear decay with  $1/L$ .

The duration of the relaxation process triggered by the deposition of a dimer is termed as the “relaxation time”  $T$  and it corresponds to the number of successive dimer

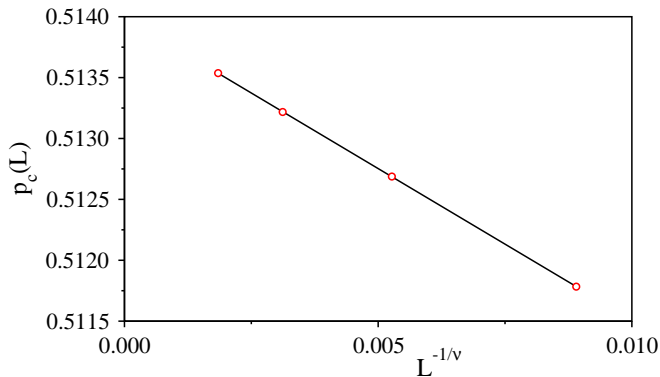


FIG. 3: Plot of the percolation threshold  $p_c(L)$  against  $L^{-1/\nu}$  with  $1/\nu = 0.756(6)$  for the lattice sizes  $L = 512, 1024, 2048,$  and  $4096$ . The asymptotic value of the percolation threshold in the limit  $L \rightarrow \infty$  has been estimated to be  $0.5140(1)$ . The data points are averages over samples ranging from  $9 \times 10^5$  for  $L = 512$  to  $8900$  for  $L = 4096$ .

displacements before a successful adsorption. This relaxation time has been measured for every dimer deposited from the beginning till the jamming state and its distribution  $D(T)$  is plotted for four different system sizes in Fig. 2. Clearly, the tail of the distribution decays exponentially in time suggesting a characteristic time of  $\approx 11.7$ , in units of dimer displacements.

### B. Percolation transition

As the surface coverage  $p$  increases, the size of the largest cluster grows monotonically. Numerically, the precise value of the percolation threshold  $p_c^\alpha$  for a specific run  $\alpha$  is determined using the bisection method [31] described as follows. We select a pair of initial values of  $p$ , namely,  $p^h$  and  $p^l$  such that there exists a global connectivity through the spanning cluster for  $p = p^h$  but not for  $p^l$ . Starting from an empty lattice the adsorption is continued till the density of occupied sites  $p = (p^h + p^l)/2$  is reached. Here, connectivity between the top and the bottom sides of the lattice is checked using the burning algorithm [23] while imposing periodic boundary condition along the horizontal direction. If the opposite sides of the lattice are connected by the same cluster,  $p^h$  is reduced to  $p$ , otherwise  $p^l$  is raised to  $p$ . In this way, the interval is iteratively bisected until  $p^h - p^l < 2/L^2$ , when  $(p^h + p^l)/2$  defines the value of  $p_c^\alpha$ . The entire procedure is then repeated for a large number of independent runs and the individual percolation thresholds are averaged to obtain the estimated percolation threshold  $p_c(L) = \langle p_c^\alpha(L) \rangle$  for the surface of size  $L$ . These values are then extrapolated to obtain the asymptotic value  $p_c$  in the limit  $L \rightarrow \infty$  using,

$$p_c(L) = p_c - AL^{-1/\nu}, \quad (1)$$

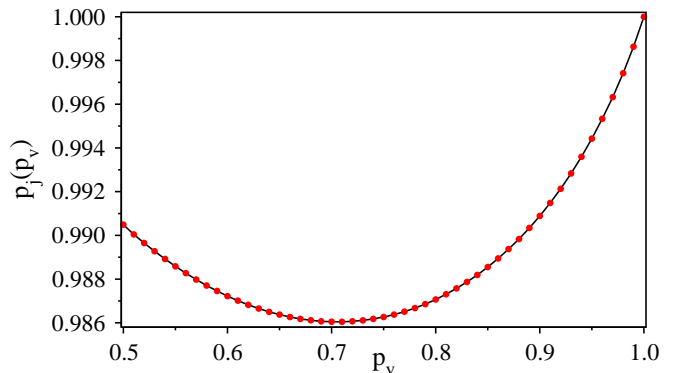


FIG. 4: For  $L = 1024$ , the jamming state coverage  $p_j(p_v)$  has been plotted against the selection probability  $p_v$  of the vertically oriented dimers. The data points are averages over (at least)  $10^5$  samples.

where  $\nu$  is known as the correlation length exponent in percolation theory and its value is  $4/3$  for random percolation in two dimensions [23, 32]. The obtained values of  $p_c(L)$  are plotted against  $L^{-1/\nu}$  in Fig. 3. Tuning the value of  $1/\nu$ , the data is found to be fit best by a straight line (using the least square fit of a straight line with minimal error) for  $1/\nu = 0.756$ . By extrapolating to the thermodynamic limit ( $L \rightarrow \infty$ ), we obtain  $p_c = 0.5140(1)$ . This value is much smaller than the value of  $p_c = 0.5618(1)$  for the RSA without relaxation [33, 34].

Qualitatively, one can try to understand the reduction in the value of percolation threshold in the following way. Let us consider a situation where a single vacant site  $P$  separates two distinct clusters connected to the top and bottom boundaries. In RSA without relaxation, it needs a dimer to be adsorbed precisely on this vacant site to connect the two. With relaxation, a dimer may be deposited at many other locations, yet due to the relaxation process another dimer may be displaced to the site  $P$  and connect the two clusters.

To investigate the critical properties of the percolation transition of RSA with relaxation, several critical exponents have been estimated. Using extensive numerical simulations, at  $p = p_c$ , we have determined the fractal dimension of the largest cluster  $d_f = 1.892(2)$ , the exponent  $\gamma/\nu = 1.790(2)$  associated with the second moment of the cluster size distribution and the fractal dimension of the shortest path  $d_l = 1.1307(5)$ . These values are consistent, within error bars, with the values known for random percolation in two dimensions, namely,  $d_f = 91/48$ ,  $\gamma/\nu = 43/24$  [23] and  $d_l = 1.13077(2)$  [35].

### C. Effect of anisotropy on jamming and percolation

So far, we have considered that the orientation of the depositing dimers is drawn at random with equal probability for horizontally and vertically oriented dimers. We

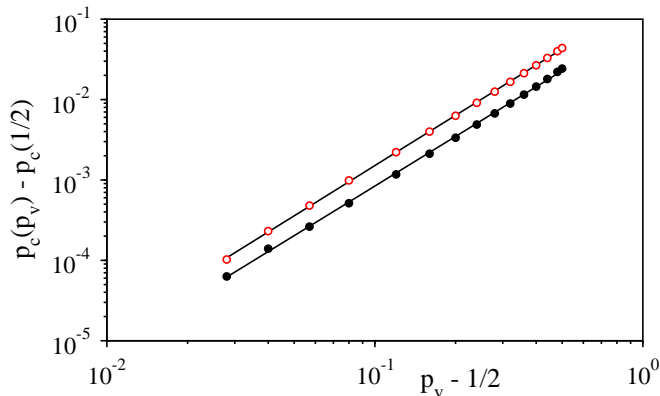


FIG. 5: Plot of the deviation of the percolation threshold  $p_c(p_v) - p_c(1/2)$  against  $p_v - 1/2$ ,  $p_v$  being the selection probability of the vertical dimers, on a log-log scale with  $p_c(1/2) = 0.5140(1)$  and  $0.5619(1)$  for the RSA with (open circles) and without (filled circles) relaxation, respectively. For each value of  $p_v$ , the  $p_c(p_v)$  in the limit of  $L \rightarrow \infty$  has been obtained using the values of  $p_c(p_v, L)$  for  $L = 256, 512, 1024, 2048$ , and  $4096$  and an extrapolation given by Eq. (1). The slopes of fitted straight lines have been measured as  $2.05(6)$  and  $2.07(7)$ , respectively. The data points are averages over samples ranging from (at least)  $1.6 \times 10^6$  for  $L = 256$  to  $5000$  for  $L = 4096$ .

now consider the anisotropic case, where these probabilities are different. More specifically, when the  $n$ -th dimer is deposited, its orientation is randomly selected with probability  $p_v$  or  $1 - p_v$  for vertical and horizontal, respectively. If the deposition attempt fails, another dimer is deposited with the same orientation but at another location (selected at random) until the adsorption is successful.

For  $p_v > 1/2$ , we observe that the clusters are elongated along the vertical direction. For this regime, the jamming state is defined as a configuration where no more vertically oriented dimer can adsorb. It turned out that the anisotropy affects significantly the value of the jamming state coverage, as shown in Fig. 4, with  $p_j = 0.99049$  for  $p_v = 1/2$ , a minimum value of  $0.98605$  for  $p_v \approx 0.71$ , and  $1.0$  for  $p_v = 1$ . This variation does not show any appreciable finite-size effects. We observed also that the exponent  $\nu_j$  that characterizes the fluctuation of the jamming state coverage remains consistently the same (within error bars) for all  $1/2 \leq p_v < 1$ . It may be noted that for the RSA without relaxation,  $p_j(p_v)$  monotonically decreases from  $0.9068$  for  $p_v = 1/2$  to  $1 - e^{-2} \approx 0.8647$  for  $p_v = 1$  [36].

The effect of anisotropy on the percolation threshold has also been studied. For a given value of the anisotropy parameter  $p_v$ , the asymptotic value of the percolation threshold  $p_c(p_v)$  has been determined using the extrapolation method described before. The deviation of  $p_c(p_v) - p_c(1/2)$  from the isotropic case has been observed to follow a power law with  $p_v - 1/2$  (Fig. 5). On a double logarithmic scale the data points fit with

an exponent =  $2.06(6)$ . Therefore, we conjecture that  $p_c(p_v) - p_c(1/2) \sim (p_v - 1/2)^2$ . Our simulation results also predict that this behavior holds for the RSA without relaxation (Fig. 5). In Table I, the values of  $p_c(p_v)$  for a few values of  $p_v$  are listed for RSA with and without relaxation.

The measured values of the critical exponents  $\nu, \gamma, d_f$  and  $d_l$  in the entire range of  $p_v$  have been found to be consistent within error bars with their respective values for random percolation in two dimensions.

#### D. Percolation through the sites occupied by similarly oriented dimers in the jamming state

Let us now distinguish the clusters of adsorbed dimers by the orientation of the corresponding dimers in the jamming state. The size  $s$  of a cluster is the number of sites occupied by the cluster. It is well known that for RSA without relaxation with  $p_v = 1/2$ , the largest among all clusters does not form a spanning path between two opposite boundaries of the lattice [37]. As, our model with relaxation dynamics enables more surface coverage, we thus address the question on whether such a spanning cluster appears with relaxation. Identifying different clusters using the burning algorithm [23] and using many independent runs, we find that the cluster size distribution  $D(s)$  follows an exponential distribution (Fig. 6(a)). Further, the average size of the largest cluster  $\langle s_{max}(L) \rangle$  is observed to grow logarithmically with the size of the system (Fig. 6(b)). These results indicate clearly that for  $p_v = 1/2$ , there exist no such spanning cluster and therefore, the system remains in the sub-critical phase of the percolation transition, when clusters are distinguished by the orientation of the dimers in the jamming state. However,  $\langle s_{max}(L) \rangle$  for the RSA with relaxation is higher in comparison to the RSA without relaxation and we see that the ratio between them asymptotically approaches to  $\approx 2.23$ .

By increasing the value of  $p_v$  from  $1/2$ , the  $\langle s_{max}(p_v) \rangle$

TABLE I: Our numerical estimates of the percolation threshold  $p_c(p_v)$  in the thermodynamic limit  $L \rightarrow \infty$ , for different values of the selection probability  $p_v$  of vertically oriented dimers for RSA with and without relaxation. Every reported value has an error bar not more than 2 in the last digit.

$p_v$	$p_c(p_v)$	
	RSA with relaxation	RSA without relaxation
0.50	0.5140	0.5619
0.58	0.5150	0.5624
0.66	0.5181	0.5640
0.74	0.5232	0.5668
0.82	0.5306	0.5708
0.90	0.5407	0.5764
0.98	0.5539	0.5840
1.00	0.5578	0.5862

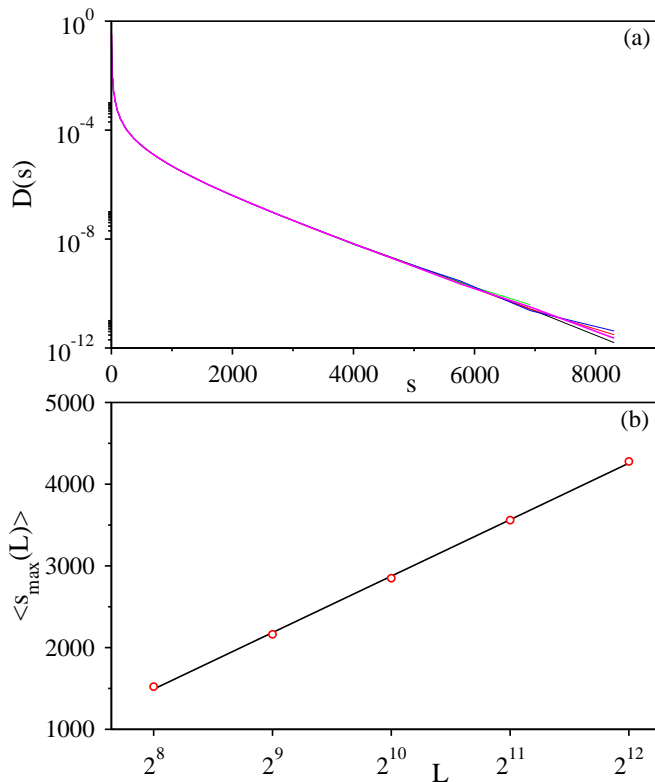


FIG. 6: Right at the jamming state for the anisotropy parameter  $p_v = 1/2$ , (a) the binned data for cluster size distribution  $D(s)$  of the vertically oriented dimers has been exhibited on a semilog scale for  $L = 256$  (black), 512 (red), 1024 (green), 2048 (blue), 4096 (magenta); (b) the average size of the largest cluster  $\langle s_{max}(L) \rangle$  for the same values of  $L$  has been plotted against  $L$  on a lin-log scale. The data points fit considerably well with a straight line indicating the logarithmic growth of the largest cluster. The results are averages over samples ranging from  $6.1 \times 10^6$  for  $L = 256$  to 6300 for  $L = 4096$ .

monotonically increases and at a critical value of  $p_v = p_{vc}$ , the largest cluster first spans the system and percolation of equal-oriented dimers occurs. In numerical simulations, imposing periodic boundary conditions along the horizontal direction, global connectivity along the vertical direction is checked through the neighboring sites occupied by vertically oriented dimers.

Tuning the value of  $p_v$  and averaging over different uncorrelated jamming state configurations for each  $p_v$ , we plot the percolation probability  $\Pi(p_v, L)$  in Fig. 7(a) for three different values of the surface sizes. The curves become more and more sharp as  $L$  is increased. All these curves intersect approximately at the same point  $[p_{vc}, \Pi(p_{vc})]$  with  $p_{vc} \approx 0.5577$  and  $\Pi(p_{vc}) \approx 0.61$ , which is slightly lower than the value 0.636454001 [38] obtained using Cardy's formula for cylindrical geometry [39]. Figure 7(b), exhibits a scaling plot of  $\Pi(p_v, L)$  against  $(p_v - p_{vc})L^{1/\nu}$ . The best data collapse for all three curves corresponds to  $p_{vc} = 0.5577(5)$  and  $1/\nu = 0.754(5)$ , im-

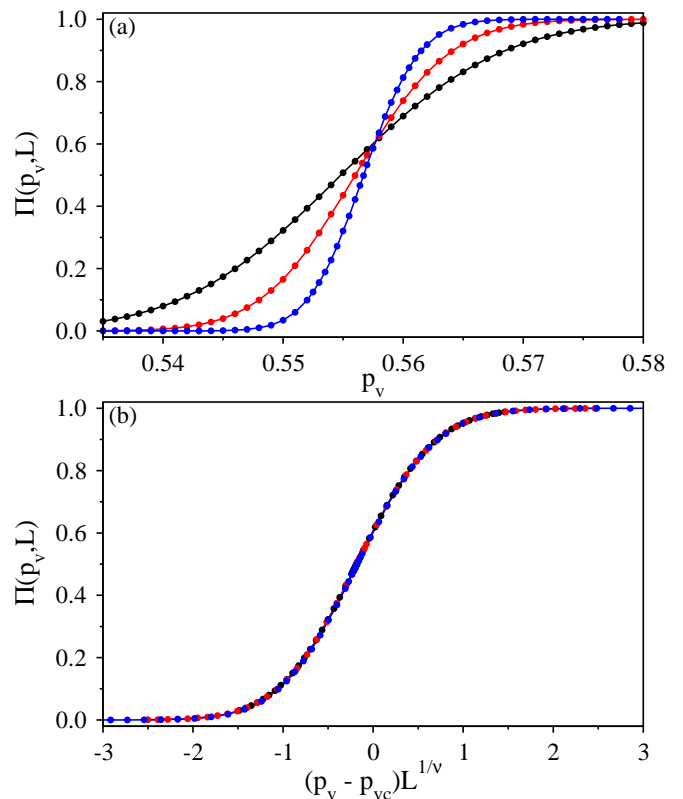


FIG. 7: (a) For  $L = 256$  (black), 512 (red) and 1024 (blue) the percolation probability  $\Pi(p_v, L)$  has been plotted with the probability of selection  $p_v$  of the vertically oriented dimers. (b) Scaling plot of the same data as in (a). A plot of  $\Pi(p_v, L)$  against  $(p_v - p_{vc})L^{1/\nu}$  using  $p_{vc} = 0.5577(5)$  and  $1/\nu = 0.754(5)$  exhibits a nice data collapse. The data points are averages over samples ranging from (at least)  $2.4 \times 10^6$  for  $L = 256$  to  $10^5$  for  $L = 1024$ .

plying a finite-size scaling form

$$\Pi(p_v, L) = \mathcal{F}[(p_v - p_{vc})L^{1/\nu}]. \quad (2)$$

Similarly, scaling analyses have been performed for the order parameter  $\Omega(p_v, L) = \langle s_{max}(p_v, L) \rangle / L^2$  and susceptibility, defined by the fluctuation of the order parameter as  $\chi(p_v, L) = \langle \Omega(p_v, L)^2 \rangle - \langle \Omega(p_v, L) \rangle^2$ . With a finite-size scaling analysis (not shown) we also find that the scaling exponents,  $\beta$  and  $\gamma$  follow within error bars the hyperscaling relation  $2\beta/\nu + \gamma/\nu = 2$  in two dimensions [23].

The second moment of the cluster size distribution  $M'_2$  is defined as  $M'_2 = \sum_k s_k^2 / L^2 - \langle s_{max} \rangle / L^2$  where,  $s_k$  being the size of the cluster  $k$ . In Fig. 8(a), the behavior of  $M'_2(p_v, L)$  has been shown for same three system sizes. By suitably scaling the abscissa and ordinate when the same data are re-plotted, an excellent data collapse is observed using  $p_{vc} = 0.5577(5)$ ,  $1/\nu = 0.754(5)$  and  $\gamma/\nu = 1.795(5)$ , indicating a scaling form

$$M'_2(p_v, L) = L^{\gamma/\nu} \mathcal{G}[(p_v - p_{vc})L^{1/\nu}]. \quad (3)$$

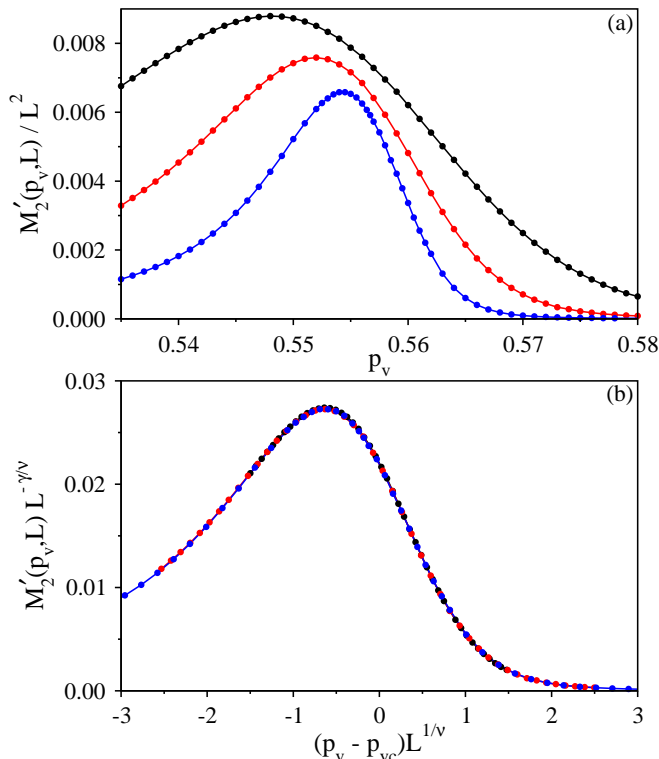


FIG. 8: (a) For  $L = 256$  (black), 512 (red) and 1024 (blue) the scaled second moment  $M'_2(p_v, L)/L^2$  has been plotted against the selection probability  $p_v$  of the vertically oriented dimers. (b) Finite-size scaling of the same data as in (a). Plot of the re-scaled second moment  $M'_2(p_v, L)L^{-\gamma/\nu}$  with the scaling variable  $(p_v - p_{vc})L^{1/\nu}$  using  $p_{vc} = 0.5577(5)$ ,  $1/\nu = 0.754(5)$  and  $\gamma/\nu = 1.795(5)$  exhibits a nice data collapse. The data points are averages over samples ranging from (at least)  $2.4 \times 10^6$  for  $L = 256$  to  $10^5$  for  $L = 1024$ .

The same set of scaling analyses have been performed for RSA without relaxation, and we obtain  $p_{vc} = 0.6056(5)$ .

#### IV. FINAL REMARKS

We introduce a model of adsorption of dimers on a two dimensional surface, with relaxation. The dimers are sequentially and irreversibly adsorbed on a square lattice at random locations by following a set of pre-

defined conditions. Most importantly, a relaxation dynamics is involved with the adsorption process. When a newly deposited dimer partially overlaps with a previously adsorbed dimer, a sequence of dimer displacements may occur to accommodate the new dimer. Every adsorption followed by the relaxation dynamics includes a pair of new occupied sites separated by a distance larger than unity and therefore, setting in spatial correlations. The effect of the relaxation dynamics and anisotropy in the orientation of the adsorbed dimers on the jamming state and percolation transition have been investigated in detail.

The percolation transition for the isotropic case occurs at a critical density of occupied sites  $p_c = 0.5140(1)$ . The increase of anisotropy,  $p_v$ , of the occurrence of vertical dimers results in an increase of the percolation threshold. In comparison to the Random Sequential Adsorption (RSA) model without relaxation, the percolation threshold in the entire range of  $p_v$  is much lower for our model with relaxation. Using extensive numerical simulations and measuring different critical exponents associated with the transition lead us to conclude that, despite the developed spatial correlations, the percolation transition always fall into the random percolation universality class.

The jamming state coverage is higher for RSA with relaxation than without relaxation. A non-monotonic variation of jamming state coverage with the strength of anisotropy  $p_v$  has been observed for RSA with relaxation. Further, separating out the vertically oriented dimers from the horizontal ones in the jamming state, a percolation transition through the cluster of sites occupied by vertically oriented dimers is observed when the control parameter  $p_v$  is tuned to the critical value  $p_{vc} = 0.5577(5)$ . Also here, the directionality does not affect the critical (universal) properties of the percolation transition.

#### Acknowledgments

S.K. and N.A.M.A. acknowledge financial support from the Portuguese Foundation for Science and Technology (FCT) under the contract no. UID/FIS/00618/2013. S.K. acknowledges senior research fellowship, provided by S. N. Bose National Centre for Basic Sciences, Kolkata, India.

[1] V. Privman, Trends in Stat. Phys. **1**, 89 (1994).  
 [2] E. Kumacheva, R. K. Golding, M. Allard, and E. H. Sargent, Adv. Matter **14**, 221 (2002).  
 [3] P. C. Lewis, E. Kumacheva, M. Allard, and E. H. Sargent, J. Dispers. Sci. Technol. **26**, 259 (2005).  
 [4] É. O'Connor, A. O'Riordan, H. Doyle, S. Moynihan, A. Cuddihy, and G. Redmond, Appl. Phys. Lett. **86**, 201114 (2005).

[5] J. W. Evans, Rev. Mod. Phys. **65**, 1281 (1993).  
 [6] S. Torquato, and F. H. Stillinger, Rev. Mod. Phys. **82**, 2633 (2010).  
 [7] C. Burda, X. Chen, R. Narayanan, and M. A. El-Sayed, Chem. Rev. **105**, 1025 (2005).  
 [8] C. L. N. Oliveira, N. A. M. Araújo, J. S. Andrade, and H. J. Herrmann, Phys. Rev. Lett. **113**, 155701 (2014).  
 [9] M. C. Bartelt and V. Privman, Int. J. Mod. Phys. B **5**,

- 2883 (1991).
- [10] V. Privman, *J. Adhesion* **74**, 421 (2000).
- [11] A. Cadilhe, N. A. M. Araújo, and V. Privman, *J. Phys.: Condens. Matter* **19**, 065124 (2007).
- [12] P. J. Flory, *J. Am. Chem. Soc.* **61**, 1518 (1939).
- [13] A. Rényi, *Publ. Math. Inst. Hung. Acad. Sci.* **3**, 109 (1958).
- [14] J. Feder, *J. Theor. Biol.* **87**, 237 (1980).
- [15] S. S. Manna and N. M. Svrakic, *J. Phys. A* **24**, L671 (1991).
- [16] D. A. King, and M. G. Wells, *Proc. R. Soc. London, Ser. A* **339**, 245 (1974).
- [17] X. C. Guo, J. M. Bradley, A. Hopkinson, and D. A. King, *Surf. Sci.* **310**, 163 (1994).
- [18] G. J. Rodgers, and J. A. N. Filipe, *J. Phys. A* **30**, 3449 (1997).
- [19] M. Cieřła, G. Pajak, R. M. Ziff, *Phys. Chem. Chem. Phys.* 2015 **17**, 24376 2015.
- [20] D. Joshi, D. Bargteil, A. Caciagli, J. Burelbach, Z. Xing, A. S. Nunes, D. E. P. Pinto, N. A. M. Araújo, J. Brujic, and E. Eiser, *Sci. Adv.* **2**, 8 (2016).
- [21] D. E. P. Pinto, and N. A. M. Araújo, *Phys. Rev. E* **98** 012125 (2018).
- [22] S. Broadbent and J. Hammersley, *Percolation processes I. Crystals and mazes*, Proceedings of the Cambridge Philosophical Society **53**, 629 (1957).
- [23] D. Stauffer and A. Aharony, *Introduction to Percolation Theory*, Taylor & Francis, (2003).
- [24] G. Grimmett, *Percolation*, Springer (1999).
- [25] M. Sahimi. *Applications of Percolation Theory*, Taylor & Francis, (1994).
- [26] M. Sahimi, *Rev. Mod. Phys.* **65**, 1393 (1993).
- [27] N. A. M. Araújo, P. Grassberger, B. Kahng, K. J. Schrenk and R. M. Ziff, *Eur. Phys. J. Special Topics* **223**, 2307 (2014).
- [28] A. A. Saberi, *Physics Reports* **578**, 1 (2015).
- [29] D. Lee, Y. S. Cho and B. Kahng, *J. Stat. Mech.* **2016**, 124002 (2016).
- [30] J. L. Jacobsen, *J. Phys. A: Math. Theor.*, **48**, 454003 (2015).
- [31] S. Kundu and S. S. Manna, *Phys. Rev. E* **95**, 052124 (2017).
- [32] P. D. Eschbach, D. Stauffer and H. J. Herrmann, *Phys. Rev. B*, **23**, 422 (1981).
- [33] N. Vandewalle, S. Galam and M. Kramer, *Eur. Phys. J. B* **14**, 407 (2000).
- [34] V. A. Cherkasova, Y. Y. Tarasevich, N. I. Lebovka and N. V. Vygornitskii, *Eur. Phys. J. B* **74**, 205 (2010).
- [35] Z. Zhou, J. Yang, Y. Deng and R. M. Ziff, *Phys. Rev. E* **86**, 061101 (2012).
- [36] P. L. Krapivsky, S. Redner, and E. Ben-Naim, *A Kinetic view of Statistical Physics*, Cambridge University Press, New York (2010).
- [37] N. I. Lebovka, N. N. Karmazina, Y. Y. Tarasevich, and V. V. Laptev, *Phys. Rev. E* **84**, 061603 (2011).
- [38] R. M. Ziff, *Phys. Rev. E* **83**, 020107(R) (2011).
- [39] J. Cardy, *J. Stat. Phys.* **125**, 1 (2006).